

## Destruction of $^{18}\text{F}$ via $^{18}\text{F}(p, \alpha)^{15}\text{O}$ burning through the $E_{\text{c.m.}}=665$ keV resonance

D. W. Bardayan,<sup>1,2</sup> J. C. Blackmon,<sup>1</sup> W. Bradfield-Smith,<sup>3</sup> C. R. Brune,<sup>2</sup> A. E. Champagne,<sup>2</sup> T. Davinson,<sup>4</sup> B. A. Johnson,<sup>5</sup> R. L. Kozub,<sup>5</sup> C. S. Lee,<sup>6</sup> R. Lewis,<sup>3</sup> P. D. Parker,<sup>3</sup> A. C. Shotter,<sup>4</sup> M. S. Smith,<sup>1</sup> D. W. Visser,<sup>3</sup> and P. J. Woods<sup>4</sup>

<sup>1</sup>Physics Division, Oak Ridge National Laboratory, Oak Ridge, Tennessee 37831

<sup>2</sup>Department of Physics and Astronomy, University of North Carolina, Chapel Hill, North Carolina 27599

<sup>3</sup>A. W. Wright Nuclear Structure Laboratory, Yale University, New Haven, Connecticut 06511

<sup>4</sup>Department of Physics and Astronomy, University of Edinburgh, Edinburgh EH9 3JZ, United Kingdom

<sup>5</sup>Physics Department, Tennessee Technological University, Cookeville, Tennessee 38505

<sup>6</sup>Department of Physics, Chung-Ang University, Seoul 156-756, South Korea

(Received 15 November 2000; published 1 May 2001)

Knowledge of the astrophysical rate of the  $^{18}\text{F}(p, \alpha)^{15}\text{O}$  reaction is important for understanding the  $\gamma$ -ray emission expected from novae and heavy-element production in x-ray bursts. The rate of this reaction is dominated at temperatures above  $\sim 0.4$  GK by a resonance near 7.08 MeV excitation energy in  $^{19}\text{Ne}$ . The  $^{18}\text{F}(p, \alpha)^{15}\text{O}$  rate has been uncertain in part because of disagreements among previous measurements concerning the resonance strength and excitation energy of this state. To resolve these uncertainties, we have made simultaneous measurements of the  $^1\text{H}(^{18}\text{F}, p)^{18}\text{F}$  and  $^1\text{H}(^{18}\text{F}, \alpha)^{15}\text{O}$  excitation functions using a radioactive  $^{18}\text{F}$  beam at the ORNL Holifield Radioactive Ion Beam Facility. A simultaneous fit of the data sets has been performed, and the best fit was obtained with a center-of-mass resonance energy of  $664.7 \pm 1.6$  keV ( $E_x = 7076 \pm 2$  keV), a total width of  $39.0 \pm 1.6$  keV, a proton branching ratio of  $\Gamma_p/\Gamma = 0.39 \pm 0.02$ , and a resonance strength of  $\omega\gamma = 6.2 \pm 0.3$  keV.

DOI: 10.1103/PhysRevC.63.065802

PACS number(s): 27.20.+n, 25.40.Cm, 25.60.-t, 26.30.+k

### I. INTRODUCTION

The observation of  $\gamma$  rays from nova ejecta would provide a rather direct test of nova models [1,2]. Immediately after a nova explosion, the most powerful  $\gamma$ -ray emission is calculated to be at energies of 511 keV and below, originating from electron-positron annihilation following the  $\beta$  decay of proton-rich radioactive nuclei produced in the explosion and Compton scattering of the annihilation radiation [3]. Because of its relatively long half-life and large abundance, the decay of  $^{18}\text{F}$  is thought to be the most important source for  $\gamma$ -ray emission during the first several hours after the explosion. The amount of  $^{18}\text{F}$  produced and transported to the nova envelope is severely constrained by its destruction rate [via the  $^{18}\text{F}(p, \alpha)^{15}\text{O}$  reaction] in the burning shells. Unfortunately, it has been found that the current uncertainties in the  $^{18}\text{F}(p, \alpha)^{15}\text{O}$  rate result in a factor of  $\sim 300$  variation in the amount of  $^{18}\text{F}$  produced in models [4]. A more precise value of the  $^{18}\text{F}(p, \alpha)^{15}\text{O}$  stellar reaction rate is thus required in order to evaluate the use of orbital detectors for observations of these  $\gamma$  rays.

Knowledge of the  $^{18}\text{F}(p, \alpha)^{15}\text{O}$  rate is also important for understanding heavy-element production in x-ray bursts, where much higher temperatures and densities are reached than in novae [5]. In these conditions, there may be a transition to heavy element production via the reaction sequence  $^{18}\text{F}(p, \gamma)^{19}\text{Ne}(p, \gamma)^{20}\text{Na}(p, \gamma)^{21}\text{Mg} \dots$  [6]. Whether there is a significant flow through this reaction sequence in x-ray bursts depends sensitively on the competition between the  $^{18}\text{F}(p, \gamma)^{19}\text{Ne}$  and  $^{18}\text{F}(p, \alpha)^{15}\text{O}$  reactions, and thus we must know their relative rates in this high-temperature astrophysical environment.

States in  $^{19}\text{Ne}$  that provide resonances for the  $^{18}\text{F}+p$  sys-

tem have been studied with both direct and indirect methods [7–12]. The  $^{18}\text{F}(p, \alpha)^{15}\text{O}$  rate is dominated in the temperature range  $0.4 \text{ GK} \leq T \leq 2.0 \text{ GK}$  by a resonance near  $E_{\text{c.m.}} = 665$  keV in  $^{19}\text{Ne}$  [7]. It was deduced from  $^1\text{H}(^{18}\text{F}, p)^{18}\text{F}$  scattering measurements that this state is an  $s$ -wave resonance in the  $^{18}\text{F}+p$  system [8,11,12] and thus must have  $J^\pi = \frac{3}{2}^+$  or  $\frac{1}{2}^+$ . The results from previous experimental studies of this state are summarized in Table I. In their investigation, Utku *et al.* [7] populated the state using the  $^{19}\text{F}(^3\text{He}, t)^{19}\text{Ne}$  reaction. They reported the total width ( $\Gamma$ ) to be  $39 \pm 10$  keV and the proton branching ratio ( $\Gamma_p/\Gamma$ ) to be  $0.37 \pm 0.04$ . In a recent report, however, Fortune and Sherr [13] have pointed out a mistake in the method by which the total width was extracted. On that basis, we have reanalyzed the data in Ref. [7] and extracted a width of  $26 \pm 10$  keV. From these corrected quantities and the assumption that the level has  $J^\pi = \frac{3}{2}^+$ , we calculate the resonance strength ( $\omega\gamma$ ) for the  $^{18}\text{F}(p, \alpha)^{15}\text{O}$  reaction to be  $4.0 \pm 1.5$  keV. Coszach *et al.* [8] found  $\Gamma = 37 \pm 5$  keV and  $\Gamma_p/\Gamma = 0.4\text{--}0.6$  by deconvoluting the  $^1\text{H}(^{18}\text{F}, p)^{18}\text{F}$  and  $^1\text{H}(^{18}\text{F}, \alpha)^{15}\text{O}$  energy spectra measured with a thick ( $200 \mu\text{g}/\text{cm}^2$ ) polyethylene target. From the measured yield of the  $^1\text{H}(^{18}\text{F}, \alpha)^{15}\text{O}$  reaction, they deduced a resonance strength of  $5.6 \pm 0.6$  keV. In a subsequent publication, Graulich *et al.* [9] used the measured total width from Ref. [8] and the proton branching ratio from Ref. [7] to calculate a resonance strength of  $5.7 \pm 0.9$  keV. Rehm *et al.* [10] extracted  $\Gamma = 13.6 \pm 4.6$  keV and  $\omega\gamma = 2.1 \pm 0.7$  keV from a measurement of the yield of the  $^1\text{H}(^{18}\text{F}, ^{15}\text{O})^4\text{He}$  reaction as a function of beam energy with a thinner ( $60 \mu\text{g}/\text{cm}^2$ ) target. This factor of 3 discrepancy in the resonance strength and 21 keV difference in resonance energy for the state resulted in a factor of 3 variation in the calculated  $^{18}\text{F}(p, \alpha)^{15}\text{O}$  rate.

TABLE I. A summary of the resonance properties from previous measurements is shown along with the best-fit results from this work.

	$E_r$ (keV)	$\Gamma$ (keV)	$\Gamma_p/\Gamma$	$\omega\gamma$ (keV)
Ref. [7]	$659 \pm 9$	$26 \pm 10^a$	$0.37 \pm 0.04$	$4.0 \pm 1.5^a$
Ref. [8]	$638 \pm 15$	$37 \pm 5$	0.4 - 0.6	$5.6 \pm 0.6$
Ref. [10]	$652 \pm 4$	$13.6 \pm 4.6$	$0.37^b$	$2.1 \pm 0.7$
Ref. [11]	$665.3 \pm 1.7$	$38.5 \pm 3.4$	$0.41 \pm 0.02$	$6.2 \pm 0.6$
Ref. [12]	$657.5 \pm 1.8$	$34.2 \pm 2.2$	$0.47 \pm 0.02$	$4.7 \pm 0.2$
This work Breit-Wigner	$664.5 \pm 0.6$	$39.7 \pm 1.9$	$0.405 \pm 0.015$	
This work $R$ matrix	$664.8 \pm 0.5$	$38.3 \pm 1.0$	$0.380 \pm 0.014$	
This work adopted	$664.7 \pm 1.6$	$39.0 \pm 1.6$	$0.39 \pm 0.02$	$6.2 \pm 0.3$

<sup>a</sup>Based on reanalysis of data in Ref. [7] as suggested in Ref. [13].

<sup>b</sup>Analysis assumed  $\Gamma_p/\Gamma=0.37$  from Ref. [7].

Subsequent experiments have clarified the situation. In a recent publication [11], we reported a measurement of the  $^1\text{H}(^{18}\text{F},p)^{18}\text{F}$  excitation function using a well-calibrated  $^{18}\text{F}$  beam and a thin ( $35 \mu\text{g}/\text{cm}^2$ ) polypropylene target. From the measured scattering yields, we deduced  $\Gamma_p/\Gamma=0.41 \pm 0.02$ ,  $\Gamma=38.5 \pm 3.4$  keV, and  $\omega\gamma=6.2 \pm 0.6$  keV. In addition, Graulich *et al.* [12] repeated the measurement of Ref. [8] with better statistics and obtained  $\Gamma_p/\Gamma=0.47 \pm 0.02$ ,  $\Gamma=34.2 \pm 2.2$  keV, and  $\omega\gamma=4.7 \pm 0.2$  keV. In the present paper, we report a measurement of the  $^1\text{H}(^{18}\text{F},\alpha)^{15}\text{O}$  excitation function which was measured simultaneously with our previously reported  $^1\text{H}(^{18}\text{F},p)^{18}\text{F}$  scattering yields [11]. A simultaneous analysis of the two data sets results in an unambiguous determination of the resonance strength of this state. In addition, from the magnitude of the measured  $^1\text{H}(^{18}\text{F},\alpha)^{15}\text{O}$  cross section, the spin and parity of the state are confirmed to be  $J^\pi=\frac{3}{2}^+$ .

## II. EXPERIMENTAL DESCRIPTION

The  $^{18}\text{F}$  beam was produced at the ORNL Holifield Radioactive Ion Beam Facility (HRIBF) by an isotope separator online-type target/ion source [14] via the  $^{16}\text{O}(\alpha, pn)^{18}\text{F}$  reaction [15]. After production, the  $^{18}\text{F}$  atoms traveled through two stages of mass analysis before being injected into the HRIBF tandem accelerator where they were accelerated to the appropriate energies for the experiment. The average beam current on target was  $2 \times 10^5$   $^{18}\text{F}$  ions per second, and a total of  $2 \times 10^{10}$   $^{18}\text{F}$  ions were incident on the target over the course of the experiment. The beam was contaminated by  $^{18}\text{O}$  ( $^{18}\text{F}/^{18}\text{O} \sim 0.1$ ), and our experiment was designed to overcome this difficulty.

The experimental configuration is shown in Fig. 1. The  $^{18}\text{F}$  beam bombarded a  $35\text{-}\mu\text{g}/\text{cm}^2$  polypropylene ( $\text{CH}_2$ )<sub>*n*</sub> foil, and the scattered protons were detected in a silicon detector array (SIDAR) [16,17]. The detectors (each having 16 radial divisions) were tilted upstream at a  $43^\circ$  angle in order to cover a large angular range ( $15^\circ \leq \theta_{\text{lab}} \leq 43^\circ$ ).

For the  $^1\text{H}(^{18}\text{F},p)^{18}\text{F}$  measurement, the recoil  $^{18}\text{F}$  ions were detected in coincidence with the scattered protons in an isobutane-filled ionization chamber which provided energy loss and total energy information for particle identification and allowed us to readily distinguish the  $^{18}\text{F}+p$  scattering

events from the more intense  $^{18}\text{O}+p$  events. Proton yields were measured at 15 beam energies between 10 and 14 MeV. The yield at each energy was determined by summing the number of coincident protons detected by the SIDAR and normalizing to the incident beam current. The proton yields are displayed in Fig. 2(a) and clearly show the presence of a resonance which interferes with the nonresonant elastic scattering. From the magnitude and shape of the scattering anomaly, the resonance must have been populated by an  $l=0$  partial wave, and thus the state must have  $J^\pi=\frac{3}{2}^+$  or  $\frac{1}{2}^+$ .

The  $^1\text{H}(^{18}\text{F},\alpha)^{15}\text{O}$  cross section was simultaneously determined by measuring the yield of  $\alpha$  particles and  $^{15}\text{O}$  ions detected in coincidence over the angular range  $\theta_{\text{c.m.}} \approx 95^\circ - 125^\circ$  as a function of bombarding energy. As shown in Fig. 1, both reaction products were detected in the SIDAR. Due to the kinematics of the reaction and our detector geometry, all of the events of interest occurred with  $\alpha$  particles being detected at lab angles greater than  $24^\circ$  and  $^{15}\text{O}$  ions less than  $19^\circ$ . The  $^1\text{H}(^{18}\text{F},\alpha)^{15}\text{O}$  events were distinguished from other coincident events by plotting (Fig. 3) the detected  $\alpha$  energy versus the heavy recoil energy. To produce this plot, a software cut was made at  $\theta_{\text{lab}}=21^\circ$ ; if a particle was detected at  $\theta_{\text{lab}} > 21^\circ$ , it was called an  $\alpha$  particle, and for  $\theta_{\text{lab}} < 21^\circ$  it was called a heavy recoil. Reactions for which

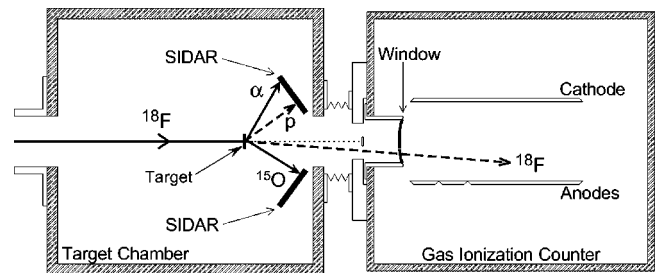


FIG. 1. Our experimental configuration is shown with the  $^{18}\text{F}$  ions impinging on a polypropylene target. For the  $^1\text{H}(^{18}\text{F},p)^{18}\text{F}$  measurement, scattered protons were detected in the SIDAR (silicon detector array) in coincidence with recoil  $^{18}\text{F}$  ions detected by the ionization counter. For the  $^1\text{H}(^{18}\text{F},\alpha)^{15}\text{O}$  measurement, both the recoil  $^{15}\text{O}$  ions and  $\alpha$  particles were detected in coincidence in the SIDAR.

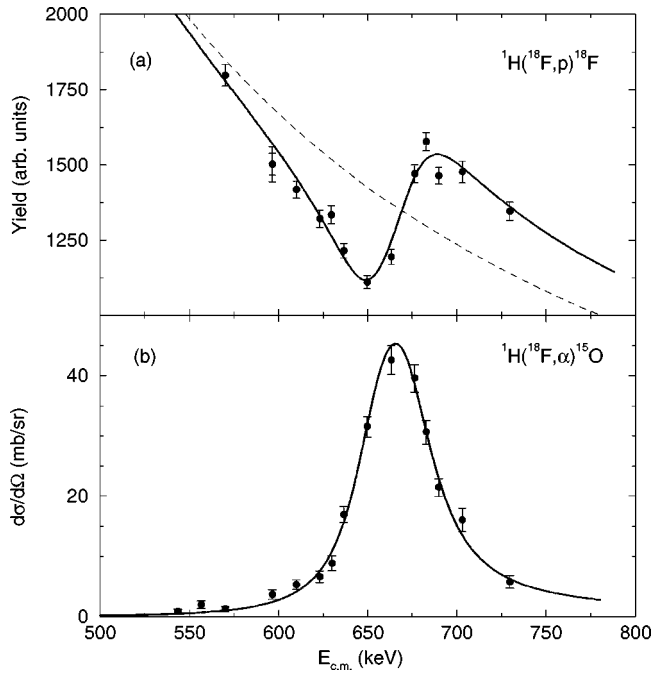


FIG. 2. (a) The normalized proton yields are plotted as a function of the average center-of-mass energy in the target. The solid curve shows the best  $R$ -matrix fit, and the dashed curve shows the expected excitation function if there were no resonances in this energy region. (b) The  $^1\text{H}(^{18}\text{F}, \alpha)^{15}\text{O}$  differential cross section in the center-of-mass system is plotted as a function of the average energy in the target. The absolute normalization was determined relative to the previously measured  $^1\text{H}(^{18}\text{O}, \alpha)^{15}\text{N}$  cross section. Because of variations in the previous  $^{18}\text{O}(p, \alpha)^{15}\text{N}$  measurements, the normalization is uncertain by 15%.

both outgoing particles were detected appear as lines of constant total energy in Fig. 3. Owing to the different  $Q$  values for the reactions, the  $^1\text{H}(^{18}\text{F}, \alpha)^{15}\text{O}$  events were readily distinguished from the more intense  $^1\text{H}(^{18}\text{O}, \alpha)^{15}\text{N}$  events.

As a further check of the events in Fig. 3 that satisfied the

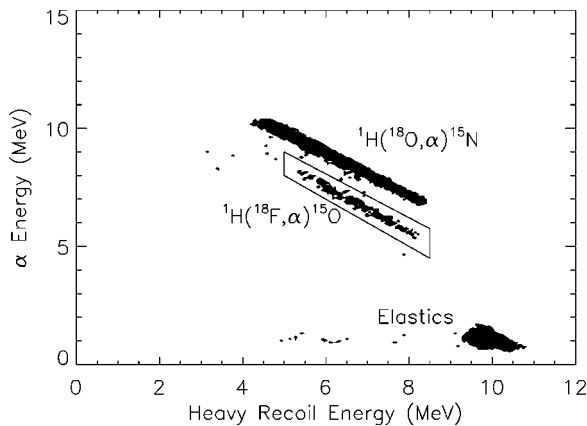


FIG. 3. The  $\alpha$ -particle energy is plotted versus the heavy recoil energy. Reactions for which both outgoing particles were detected appear as lines of constant total energy. Owing to the different  $Q$  values for the reactions, the  $^1\text{H}(^{18}\text{F}, \alpha)^{15}\text{O}$  events were readily distinguished from  $^1\text{H}(^{18}\text{O}, \alpha)^{15}\text{N}$  events. A gate is shown around the events of interest.

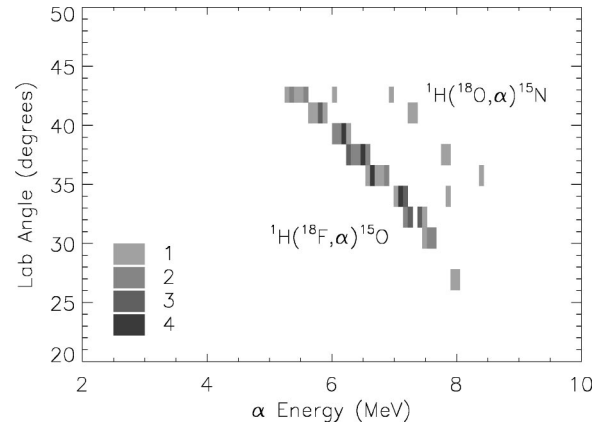


FIG. 4. The  $\alpha$  angle is plotted as a function of  $\alpha$  energy for those events that fall inside the energy gate shown in Fig. 3. This was done to ensure that the correct kinematical relationship was satisfied and to reject any  $^1\text{H}(^{18}\text{O}, \alpha)^{15}\text{N}$  events which leak into the energy gate.

$^1\text{H}(^{18}\text{F}, \alpha)^{15}\text{O}$  total energy requirement (shown inside the gate in Fig. 3), the lab angles of the detected  $\alpha$  particles were plotted versus their energies. An example of this is shown in Fig. 4. This was done to ensure that the selected events satisfied the correct kinematical relationship, and allowed the rejection of any remaining  $^1\text{H}(^{18}\text{O}, \alpha)^{15}\text{N}$  events. In addition, the coplanarity condition (i.e., the requirement that the  $\alpha$  particle and the  $^{15}\text{O}$  ion were separated by an azimuthal angle of  $\Delta\phi = 180^\circ \pm 60^\circ$ , where  $60^\circ$  was the angular range covered by a single SIDAR strip) was checked for all of the selected events.

The differential cross section in the center-of-mass system [shown in Fig. 2(b)] was calculated from the observed yield at each energy as

$$\frac{d\sigma}{d\Omega} = \frac{Y(E)}{IN \sum_s \Delta\Omega_s \varepsilon_s}, \quad (1)$$

where  $Y(E)$  was the number of  $\alpha$  particles from the  $^1\text{H}(^{18}\text{F}, \alpha)^{15}\text{O}$  reaction detected in coincidence with an  $^{15}\text{O}$  recoil,  $I$  was the number of  $^{18}\text{F}$  ions incident on target,  $N$  was the number of target atoms ( $^1\text{H}$ ) per unit area,  $\Delta\Omega_s$  was the solid angle covered by a SIDAR strip in the center-of-mass system,  $\varepsilon_s$  was the coincidence efficiency of that strip. The sum was over all SIDAR strips with  $\theta_{\text{lab}} > 24^\circ$ , since only  $\alpha$  particles detected in these strips could physically have a recoil  $^{15}\text{O}$  ion detected in coincidence. The solid angle subtended by each strip was determined via the use of a calibrated  $^{244}\text{Cm}$  source and agreed with calculations within 1%. The target thickness ( $35 \pm 4 \mu\text{g}/\text{cm}^2$ ) was determined by measuring the energy loss of  $\alpha$  particles traversing the foil. The relative number of  $^{18}\text{F}$  ions incident on target at each energy was determined from the amount of  $^{18}\text{F}$  that was scattered from the carbon in the target and detected by the ionization counter. The coincidence efficiency of each strip was calculated from kinematics and the known detector geometry. Equation (1) assumes that the center-of-mass angu-

lar distribution is isotropic, as would result from an  $l=0$  resonance. Further justification for Eq. (1) comes from Ref. [8] where angular distribution measurements for this resonance were found to be isotropic, and our measured resonant angular distribution was also consistent with this isotropy assumption. For the points far from the resonance energy (e.g., for the measurements near  $E_{c.m.}=550$  keV), isotropy may not be a valid assumption.

While the relative normalization of the cross section measurements in Fig. 2(b) was well determined, deducing the absolute normalization was not trivial due to uncertainties in the hydrogen content of the target and in the efficiency of the detector used for beam current measurement. In order to minimize the effect of these uncertainties, the absolute normalization of the cross section was determined by comparing the observed yields (with appropriate kinematic corrections) with those from the  ${}^1\text{H}({}^{18}\text{O},\alpha){}^{15}\text{N}$  reaction which was measured simultaneously. The relative intensities of the  ${}^{18}\text{F}$  and  ${}^{18}\text{O}$  beams were measured with  $<1\%$  statistical uncertainty by counting the relative numbers of  ${}^{18}\text{F}$  and  ${}^{18}\text{O}$  ions scattered from carbon in the target and detected by the ionization counter and then correcting for the different atomic numbers of fluorine and oxygen. The  ${}^1\text{H}({}^{18}\text{F},\alpha){}^{15}\text{O}$  differential cross section was normalized to that of  ${}^1\text{H}({}^{18}\text{O},\alpha){}^{15}\text{N}$  at  $E_{c.m.}=663$  keV, because at that energy the  ${}^1\text{H}({}^{18}\text{O},\alpha){}^{15}\text{N}$  cross section is isotropic [18]. The average of the previously measured values for the  ${}^{18}\text{O}(p,\alpha){}^{15}\text{N}$  cross section [18–20] is  $20\pm 3$  mb/sr, where the uncertainty was chosen to overlap the measured values. Using this value for the  ${}^{18}\text{O}(p,\alpha){}^{15}\text{N}$  cross section, the normalization of the measured  ${}^{18}\text{F}(p,\alpha){}^{15}\text{O}$  cross section at  $E_{c.m.}=663$  keV was fixed to be  $42.6\pm 2.4$  mb/sr. Since the relative normalization of the points was known, fixing the absolute value of the cross section at one energy determined the values at all energies. Because the  ${}^{18}\text{O}(p,\alpha){}^{15}\text{N}$  cross section is uncertain by  $\pm 15\%$ , however, the absolute normalization of our cross section is also uncertain by  $\pm 15\%$ .

### III. SIMULTANEOUS FIT OF THE DATA SETS

A simultaneous fit of the measured  ${}^1\text{H}({}^{18}\text{F},p){}^{18}\text{F}$  and  ${}^1\text{H}({}^{18}\text{F},\alpha){}^{15}\text{O}$  excitation functions was performed. For the  ${}^1\text{H}({}^{18}\text{F},p){}^{18}\text{F}$  data set, two different formalisms were used [11]. The first used the Breit-Wigner methodology detailed in Blatt and Biedenharn [21], and the second utilized the  $R$ -matrix code MULTI [22]. Assuming a  $J^\pi = \frac{3}{2}^+$  resonance, the theoretical cross section was integrated over the angles covered by the SIDAR and averaged over the energy loss in the target.

The  ${}^1\text{H}({}^{18}\text{F},\alpha){}^{15}\text{O}$  data were fitted with the standard formula for an isolated isotropic resonance [23]

$$\frac{d\sigma}{d\Omega} = \frac{1}{4} \chi^2 \omega \frac{\Gamma_p(E)\Gamma_\alpha(E)}{(E-E_r)^2 + [\Gamma(E)/2]^2}, \quad (2)$$

where  $\omega$  is the statistical factor depending only on the spins of the target, projectile, and resonant state,  $\Gamma = \Gamma_\alpha + \Gamma_p$ , and the energy dependences of the widths were obtained by scaling with the penetrabilities [24]. The differential cross sec-

tion was averaged over the energy loss in the target. Because the absolute normalization of the  ${}^1\text{H}({}^{18}\text{F},\alpha){}^{15}\text{O}$  excitation function was somewhat uncertain, the normalization of Eq. (2) was allowed to vary as a free parameter in the simultaneous fit [the fit was later repeated with a fixed normalization (see below)]. Therefore, there were five fit parameters: the normalization of the  ${}^1\text{H}({}^{18}\text{F},p){}^{18}\text{F}$  fitting function, the normalization of the  ${}^1\text{H}({}^{18}\text{F},\alpha){}^{15}\text{O}$  fitting function, the resonance energy ( $E_r$ ), the total width ( $\Gamma$ ), and the proton branching ratio ( $\Gamma_p/\Gamma$ ). Because the normalization of the  ${}^1\text{H}({}^{18}\text{F},\alpha){}^{15}\text{O}$  fit was allowed to vary, the proton branching ratio was constrained only by the  ${}^1\text{H}({}^{18}\text{F},p){}^{18}\text{F}$  data, while the resonance energy and total width were constrained by both data sets. The best fit results are shown in Table I, and the best fit is plotted in Fig. 2. The quoted uncertainties in the best fit results are purely statistical in nature, and the resonance parameters from the two fitting methods agree at the  $1\sigma$  level. We, therefore, adopt resonance parameters that are the average of the results from the two fitting methods.

A number of systematic uncertainties were carefully considered. There was no appreciable target degradation or dead time during the experiment. The measurement at 11.5 MeV ( $E_{c.m.}=597$  keV) was repeated near the end of the run ( $\sim 26$  h of beam on target between measurements) to test the reproducibility of the system and found to lie within the  $1\sigma$  uncertainties of the  ${}^1\text{H}({}^{18}\text{F},p){}^{18}\text{F}$  measurements. A similar comparison for the  ${}^1\text{H}({}^{18}\text{F},\alpha){}^{15}\text{O}$  data was not possible because of the low cross section at that energy and the significantly shorter duration of the first run at that energy. Uncertainties in the beam energy calibration [25] were recently checked [17] and found to be negligible. The best-fit results showed a mild dependence on the beam energy loss in the target used in the fitting routine. The energy loss of  $\alpha$  particles in the target was measured before and after the experiment using a  ${}^{244}\text{Cm}$  source. As in our previous experiments [17], there was no observable change in target composition. The energy loss was then converted to an expected energy loss for the  ${}^{18}\text{F}$  ions and found to be  $490\pm 50$  keV. This energy loss was consistent with the observed energy spread of the detected protons from the  ${}^1\text{H}({}^{18}\text{F},p){}^{18}\text{F}$  reaction. In the fitting routine, the energy loss was varied by its uncertainty, and the best-fit results changed by 1.5 keV for the resonance energy, by 1.2 keV for the total width, and by 0.012 for the ratio of  $\Gamma_p/\Gamma$ .

We arrive at uncertainties in our adopted resonance parameters by combining in quadrature the uncertainties of our best-fit results with the systematic uncertainties mentioned above. We therefore obtain  $E_r = 664.7\pm 1.6$  keV,  $\Gamma = 39.0\pm 1.6$  keV, and  $\Gamma_p/\Gamma = 0.39\pm 0.02$ . These agree with those obtained originally in our analysis of the  ${}^1\text{H}({}^{18}\text{F},p){}^{18}\text{F}$  data alone [11]. Our results also agree with those reported in Utku *et al.* [7] and agree with Refs. [8,12] for the total width and proton branching ratio. However, our findings for the width, resonance energy, and proton branching ratio do not agree at the  $1\sigma$  level with those in Rehm *et al.* [10] and do not agree with the resonance energies found in Refs. [8,12]. From our resonance properties, we calculate the proton partial width to be  $15.2\pm 1.0$  keV which agrees with that recently calculated by Fortune and Sherr [13]. Also, we calculate the resonance

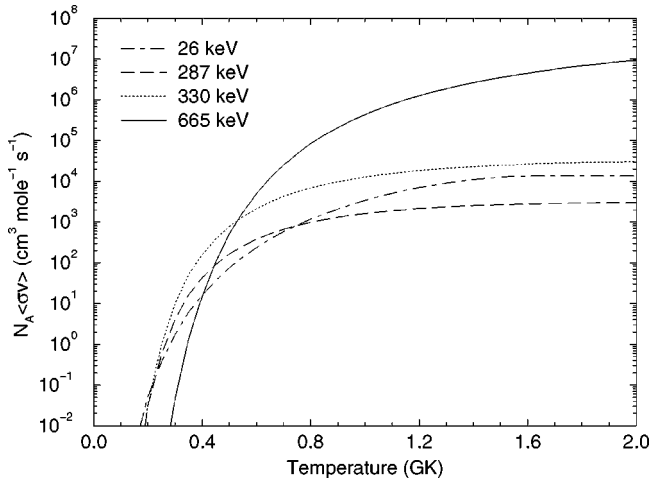


FIG. 5. The contributions of resonances in  $^{19}\text{Ne}$  to the  $^{18}\text{F}(p,\alpha)^{15}\text{O}$  rate are shown as a function of stellar temperature. The contribution of the 665-keV resonance was calculated from the adopted resonance parameters listed in Table I. The contributions from other resonances were taken from Ref. [7]. The 665-keV resonance dominates the  $^{18}\text{F}(p,\alpha)^{15}\text{O}$  reaction rate at temperatures above  $\sim 0.4$  GK. Higher energy resonances provide negligible contributions in the temperature range shown [26].

strength for the  $^{18}\text{F}(p,\alpha)^{15}\text{O}$  reaction to be  $\omega\gamma = 6.2 \pm 0.3$  keV. It is also possible to derive a value for the resonance strength based upon fitting the  $^1\text{H}(^{18}\text{F},\alpha)^{15}\text{O}$  data with Eq. (2) without taking the absolute normalization to be a free parameter. In this case, we obtain  $\omega\gamma = 6.0 \pm 1.0$  keV with the larger uncertainty resulting from the uncertainty in the absolute normalization.

From the magnitude of the  $^1\text{H}(^{18}\text{F},\alpha)^{15}\text{O}$  cross section, we can eliminate the possibility that the resonance has  $J^\pi = \frac{1}{2}^+$ . The maximum cross section possible for a  $\frac{1}{2}^+$  resonance at this energy from Eq. (2) is 27 mb/sr. This is much smaller than the observed cross section, and we therefore conclude that the observed resonance must have  $J^\pi = \frac{3}{2}^+$ .

#### IV. ASTROPHYSICAL IMPLICATIONS AND CONCLUSIONS

With these improved values for the resonance parameters, we show in Fig. 5 a calculation of the contribution of the  $\frac{3}{2}^+$  resonance to the  $^{18}\text{F}(p,\alpha)^{15}\text{O}$  stellar reaction rate. Because

our measurement has resolved the discrepancy in the values of these resonance properties, we have removed an uncertainty in the  $^{18}\text{F}(p,\alpha)^{15}\text{O}$  rate which spanned a factor of 3 at high temperatures. The total rate at temperatures below 0.4 GK is still uncertain because of the uncertain properties of lower energy states in  $^{19}\text{Ne}$  [26]. As our adopted resonance properties are very similar to those reported in Ref. [7], we support the conclusions in that paper that the  $^{18}\text{F}(p,\alpha)^{15}\text{O}$  rate is much faster than the  $^{18}\text{F}(p,\gamma)^{19}\text{Ne}$  rate in novae and x-ray bursts. The  $^{18}\text{F}(p,\alpha)^{15}\text{O}$  reaction is therefore the dominant destruction mechanism for  $^{18}\text{F}$  in these stellar explosions.

In conclusion, the  $^{18}\text{F}(p,\alpha)^{15}\text{O}$  stellar reaction rate has been uncertain, in part because of discrepant results from previous measurements [7,8,10] concerning the properties of a resonance near 7.08 MeV in  $^{19}\text{Ne}$ . Those measurements differed by as much as a factor of 3 in their adopted widths and by as much as 21 keV in their excitation energy for the state. By measuring the  $^1\text{H}(^{18}\text{F},p)^{18}\text{F}$  and  $^1\text{H}(^{18}\text{F},\alpha)^{15}\text{O}$  excitation functions with a thin target and a high-resolution  $^{18}\text{F}$  beam, we were able to determine the properties of this resonance with a greater precision than had been achieved previously. Our results for the total width and resonance strength clearly favor those found in Refs. [7,8] over the one in Ref. [10]. While our measurement has reduced the uncertainty in the  $^{18}\text{F}(p,\alpha)^{15}\text{O}$  rate in the temperature range  $0.4 \text{ GK} \leq T \leq 2.0 \text{ GK}$  to less than 10%, the rate is still uncertain at temperatures outside this range owing to the uncertain properties of other resonances in  $^{19}\text{Ne}$ . Further work with  $^{18}\text{F}$  beams is planned at the HRIBF in order to address these uncertainties.

#### ACKNOWLEDGMENTS

We thank the staff of the HRIBF whose hard work made this experiment possible. Oak Ridge National Laboratory is managed by UT-Battelle, LLC, for the U.S. Department of Energy under Contract No. DE-AC05-00OR22725. This work was also supported in part by the U.S. Department of Energy under Contract Nos. DE-FG02-91ER-40609 with Yale University, DE-FG02-96ER40955 with Tennessee Technological University, and DE-FG02-97ER41041 with the University of North Carolina at Chapel Hill, and by the Korea Research Foundation Grant No. KRF 2000-015-DP0084.

- 
- [1] M. D. Leising and D. D. Clayton, *Astrophys. J.* **323**, 159 (1987).  
 [2] M. J. Harris, J. E. Naya, B. J. Teegarden, T. L. Cline, N. Gehrels, D. M. Palmer, R. Ramaty, and H. Seifert, *Astrophys. J.* **522**, 424 (1999).  
 [3] M. Hernanz, J. José, A. Coc, J. Gómez-Gomar, and J. Isern, *Astrophys. J. Lett.* **526**, L97 (1999).  
 [4] A. Coc, M. Hernanz, J. José, and J.-P. Thibaud, *Astron. Astrophys.* **357**, 561 (2000).  
 [5] R. E. Taam, S. E. Woosley, T. A. Weaver, and D. Q. Lamb, *Astrophys. J.* **413**, 324 (1993).  
 [6] A. E. Champagne and M. Wiescher, *Annu. Rev. Nucl. Part. Sci.* **42**, 39 (1992).  
 [7] S. Utku *et al.*, *Phys. Rev. C* **57**, 2731 (1998); **58**, 1354(E) (1998).  
 [8] R. Coszach *et al.*, *Phys. Lett. B* **353**, 184 (1995).  
 [9] J.-S. Graulich *et al.*, *Nucl. Phys.* **A626**, 751 (1997).  
 [10] K. E. Rehm *et al.*, *Phys. Rev. C* **52**, R460 (1995); **53**, 1950 (1996).  
 [11] D. W. Bardayan *et al.*, *Phys. Rev. C* **62**, 042802(R) (2000).  
 [12] J.-S. Graulich *et al.*, *Phys. Rev. C* **63**, 011302(R) (2001).  
 [13] H. T. Fortune and R. Sherr, *Phys. Rev. C* **61**, 024313 (2000).

- [14] G. D. Alton and J. R. Beene, *J. Phys. G* **24**, 1347 (1998).
- [15] R. F. Welton *et al.*, *Nucl. Phys. A* (to be published).
- [16] D. W. Bardayan *et al.*, *Phys. Rev. Lett.* **83**, 45 (1999).
- [17] D. W. Bardayan *et al.*, *Phys. Rev. C* **62**, 055804 (2000).
- [18] H.-B. Mak, H. C. Evans, G. T. Ewan, and J. D. MacArthur, *Nucl. Phys.* **A304**, 210 (1978).
- [19] H. Lorenz-Wirzba, P. Schmalbrock, H. P. Trautvetter, M. Wiescher, C. Rolfs, and W. S. Rodney, *Nucl. Phys.* **A313**, 346 (1979).
- [20] N. S. Christensen, F. Jensen, F. Besenbacher, and I. Stensgaard, *Nucl. Instrum. Methods Phys. Res. B* **51**, 97 (1990).
- [21] J. M. Blatt and L. C. Biedenharn, *Rev. Mod. Phys.* **24**, 258 (1952).
- [22] R. O. Nelson, E. G. Bilpuch, and G. E. Mitchell, *Nucl. Instrum. Methods Phys. Res. A* **236**, 128 (1985).
- [23] C. E. Rolfs and W. S. Rodney, *Cauldrons in the Cosmos* (The University of Chicago Press, Chicago, 1988).
- [24] D. W. Bardayan and M. S. Smith, *Phys. Rev. C* **56**, 1647 (1997).
- [25] D. K. Olsen, K. A. Erb, C. M. Jones, W. T. Milner, D. C. Weisser, and N. F. Ziegler, *Nucl. Instrum. Methods Phys. Res. A* **254**, 1 (1987).
- [26] N. Shu *et al.* (unpublished).